INSTITUTE FOR SUSTAINABLE ENERGY, UNIVERSITY OF MALTA

SUSTAINABLE ENERGY 2013:
THE ISE ANNUAL CONFERENCE
Thursday 21st March 2013, Dolmen Hotel, Qawra, Malta

CONTROL OF A DOUBLY FED INDUCTION MACHINE IN A WIND ENERGY CONVERSION SYSTEM

K. Scicluna, C. Spiteri-Staines and M. Apap
Department of Industrial Electrical Power Conversion,
University of Malta, Msida, MSD2080, Malta,
Corresponding Author E-mail: kris.scicluna@um.edu.mt

ABSTRACT: This paper presents research done on the closed-loop control of the Doubly Fed Induction Machine (DFIM) applied to a Wind Energy Conversion System (WECS). Basic generator configurations used in wind energy systems, mainly fixed-speed and adjustable speed generators are discussed. A suitable Stator Flux Oriented (SFO) control topology for the DFIM is shown with which it is possible to control the stator active and reactive power. The control system designed was implemented on an experimental rig which emulates the behaviour of a practical WECS. A brief overview of sensorless algorithms is also presented; these algorithms are used to provide rotor speed/position estimates in the absence of a speed sensor. Practical results in both sensored and sensorless operation are shown including measurements for rotor currents, stator active/reactive power and rotor speed/position estimates.

Keywords: Doubly Fed Induction Machine, Vector Control, Sensorless

1 INTRODUCTION

The total energy generated from wind systems has been on the rise over the last decade. A report compiled by the World Wind Energy Association states that in the first half of 2011 the worldwide wind capacity had increased by 18.4 GW which was expected to increase to 43.9 GW till the end of the year. China was the worldwide leader as it contributed to 43% of the newly increased wind capacity. The total worldwide wind capacity as of June 2011 was 215 GW [1].

Most of the modern wind turbines use a Doubly Fed Induction Machine (DFIM) to generate electricity. As a result of this the DFIM is one of the most widespread type of electrical machines [2] used in industrial applications such as Wind Energy Conversion Systems (WECS). There are several advantages in using the DFIM over other machine configurations such as: increased turbine energy capture capability, reduced stresses on the mechanical structure, diminished acoustic noise and having active and reactive powers which are more controllable in terms of grid integration [3].

2 WIND ENERGY CONVERSION SYSTEMS

DFIM machines became widespread with the introduction of variable speed wind turbines which gradually replaced fixed-speed systems. The performance of fixed-speed wind turbines is heavily dependent on mechanical features such as pitch control time constants and main breaker maximum switching rate. Variable speed wind turbines make use of Adjustable Speed Generators (ASGs) which have a number of advantages compared to Fixed Speed Generators (FSGs) [4]:

- Cost effectiveness and simpler pitch control.
- Reduction in mechanical stresses as wind can be absorbed as energy and stored in the mechanical inertia of the turbine.
- Reduction in torque pulsations which results in improved power quality due to the less flickering involved.
- Overall system efficiency is improved due to Maximum Power Point Tracking (MPPT) by which maximum power can be achieved over a wide range of speeds.

An ASG configuration can be implemented either as a Direct-in-Line ASG system using a synchronous generator or as a Doubly Fed Induction Generator ASG system. The advantages associated with the latter system include [4, 5, 6]:

- The power converter is connected to the rotor windings, and the rating of the converter is proportional to the slip at which the machine is operated. This results in reduced power converter cost.
- Reduced cost for the power converter and EMI filters.
- Overall improved system efficiency in the range of 2-3%.
- Power factor control can be implemented at a lower cost since the converter has to provide

only excitation energy.

The DFIM in Wind Energy Conversion Systems (WECS) is usually driven through the Scheribius scheme illustrated in Figure 1. This topology allows for power flow in both directions and four quadrant operation of the DFIM [5]. The Scheribius Drive Scheme applied to the DFIM is characterized by [2], [6]:

- Operation below, through and above synchronous speed. The speed range is only restricted by the rotor-voltage ratings of the DFIG.
- Low distortion on stator and rotor currents.
- Independent control of the generator torque and rotor excitation.
- Control over the system power factor.

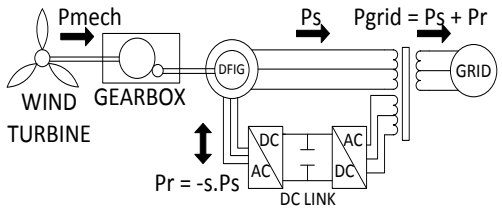

Figure 1: Scheribus Drive applied to WECS

3 VECTOR CONTROL

The basic mathematical model of the DFIM driven by wind energy is properly described in literature [2, 4, 5, 7, 8]. Such basic models take into consideration various assumptions in order to minimize computational times or to eliminate parameters which are difficult to measure in practice. These assumptions include neglecting the effects of aerodynamic efficiency, shaft stiffness and crowbar effect. Unless an in depth analysis of these parameters is carried out in advanced modelling of a WECS the effects on the overall DFIM performance remain uncertain [9].

The DFIM is being operated with a Stator Flux Oriented (SFO) vector control algorithm and a rotor side matrix converter (Figure 2). The SFO vector control theory shall not be covered in this paper as it is adequately covered in literature [3, 5, 6, 10-13]. The control algorithm uses information on the present state of the currents, voltages and rotor speed/position to control the three phase rotor currents. The reference currents in the vector control environment (Figure 2) are given in terms of i_{Rd} and i_{Rq} which are the rotor currents in the dq-frame. The transformation to the dq-frame is a mathematical operation by which the stationary rotor frame is shifted by an angle θ_{sl} which is the derivative of the slip frequency ω_{sl}. The currents in the dq-frame are related to the RMS value of the three phase rotor currents $i_{R_{a,b,c}}$ through (1).

$$i_{R_{a,b,c}} = \sqrt{\frac{i_{R_d}^2 + i_{R_q}^2}{2}} \qquad (1)$$

It is convenient to express the rotor currents in the dq-frame as these are directly proportional to the Stator Active Power (P) and Stator Reactive Power (Q) as shown in (2) and (3).

$$P = -3\frac{L_O}{L_S} i_{R_q} \Psi_s \omega_e \qquad (2)$$

$$Q = -3\left(\frac{\Psi_s v_s}{L_s} - \frac{L_O}{L_S} v_S i_{R_d}\right) \qquad (3)$$

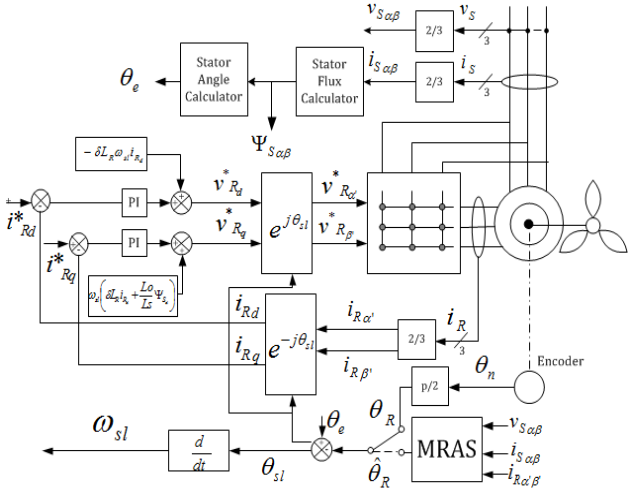

Figure 2: SFO vector control environment

4 SENSORLESS CONTROL

The SFO vector control algorithm requires information on the present state of the following DFIM parameters in order to operate correctly:

- Stator voltages v_{Sa},v_{Sb} and v_{Sc}
- Stator currents i_{Sa},i_{Sb} and i_{Sc}
- Rotor currents i_{Ra},i_{Rb} and i_{Rc}
- Rotor speed and position

The voltages and currents in a practical system are measured accurately through appropriate electronic transducers. The rotor speed and position are measured through a speed sensor, such as a tachogenerator or encoder which is mechanically coupled with the shaft of the generator. Hence the speed sensor is subject to vibrations and mechanical stresses present in the shaft which make it prone to failure in an otherwise robust system. The elevated costs associated with repairing the speed sensor in a

wind turbine have given rise to the extensive research in the field of sensorless control.

The aim of sensorless control is to replicate the control performance obtained with the sensored SFO vector control system without using a speed sensor. There are numerous techniques for obtaining speed and position estimates, most of which use information from the remaining sensors to estimate the required values. In this paper the results obtained using a model-based system known as Model Reference Adaptive System (MRAS) [14-18] are presented to show the validity of sensorless algorithms. The MRAS algorithm (Figure 3) receives the system voltages/currents at its inputs and outputs estimates for the rotor angular frequency ω_R and rotor position θ_R.

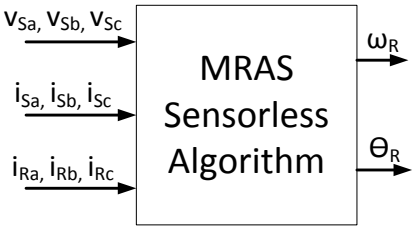

Figure 3: High-level MRAS Diagram

5 EXPERIMENTAL RESULTS

The results presented in this section are for a DFIM with system parameters as described in Table 1. The system is being driven by a DC drive at a sub-synchronous speed of 1300 rpm.

Table 1: DFIM Parameters

Parameter	Stator	Rotor
Power	1.5 kW	-
Phase voltage, current	210 V, 4.5A	150 V, 3.7 A
Resistance	1.25 Ω	1.60 Ω
Frequency	50 Hz	-
Leakage Inductance	10.83 mH	1.54 mH
Mutual Inductance	143.42 mH	
Turns Ratio (stator to rotor)	1.32	

The reference currents are set at i_{Rd} = 2.82 A and i_{Rq} = 2.39 A which correspond to rated stator operation. Assuming a 'd' current of 2.82 A has been setup during magnetization through the rotor, a 'q' current step reference of 2.39 A results in the performance shown in Figure 4.

Since the dq-frame currents have been calculated for rated stator conditions, when the step on the 'q' current is applied the Stator Active Power (P) reaches the rated value of 1.5 kW (Figure 5). The choice of the reference currents also results in a low Stator Reactive Power (Q) which at steady state is approximately equal to 0 VAr resulting in a power factor value close to unity.

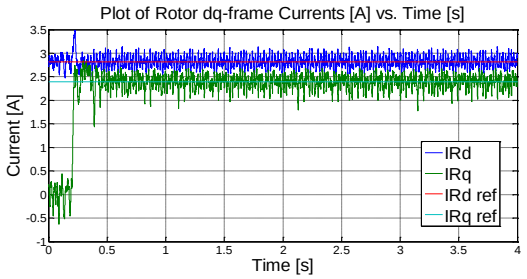

Figure 4: Plot of Rotor dq-frame Currents [A] vs. Time [s] in Sensored mode, i_{Rd}=2.82 A and i_{Rq} = 2.39 A at 1300 rpm.

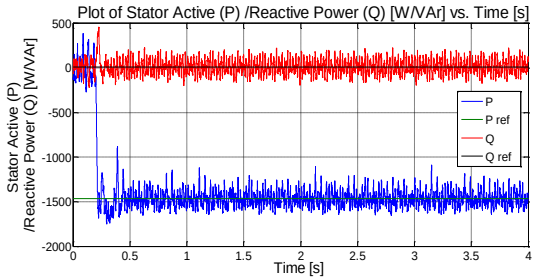

Figure 5: Plot of Stator Power (P) / Reactive Power (Q) [W / VAr] vs. Time [s] in Sensored mode, i_{Rd}=2.82 A and i_{Rq} = 2.39 A at 1300 rpm.

In the case of the sensorless mode of operation the reference step on the 'q' current has been delayed by a first order low-pass filter with a time constant of 0.4 s. This has been done to attenuate the torque pulsation associated with an increase in the 'q' current. The rotor dq-frame currents in sensorless mode are shown in Figure 6. The Stator Active Power (P) and the Stator Reactive Power (Q) in sensorless mode are shown in Figure 7.

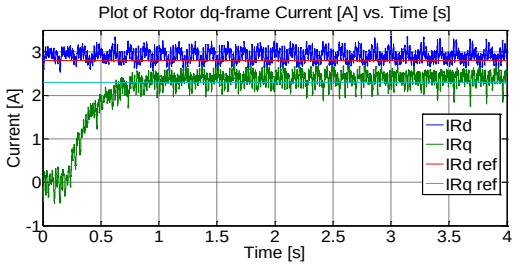

Figure 6: Plot of Rotor dq-frame Currents [A] vs. Time [s] in Sensorless mode, i_{Rd}=2.82 A and i_{Rq} = 2.39 A at 1300 rpm.

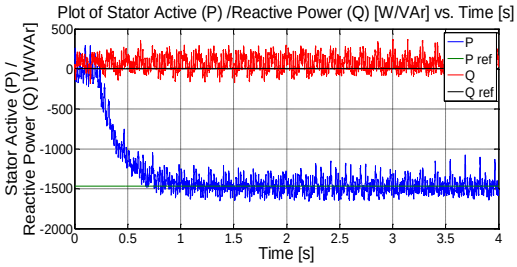

Figure 7: Plot of Stator Power (P) / Reactive Power (Q) [W / VAr] vs. Time [s] in Sensorless mode, i_{Rd}=2.82 A and i_{Rq} = 2.39 A at 1300 rpm.

The actual/estimated rotational speed and position are shown in Figures 8 and 9 respectively. The currents, stator power and estimates behave similarly through a wide speed range of the DFIM which for this experimental setup was taken between 1000 rpm to 1700 rpm. The actual/estimated rotor speeds for this range are shown in Figure 10.

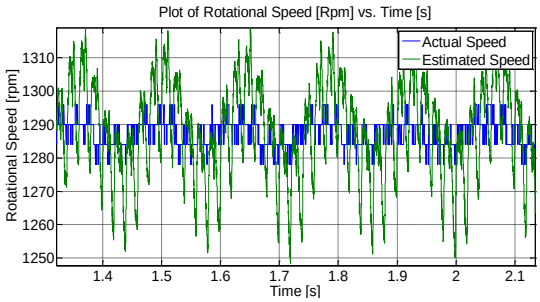

Figure 8: Plot of Rotational Speed [rpm] vs. Time [s] in Sensorless mode, i_{Rd}=2.82 A and i_{Rq} = 2.39 A at 1300 rpm.

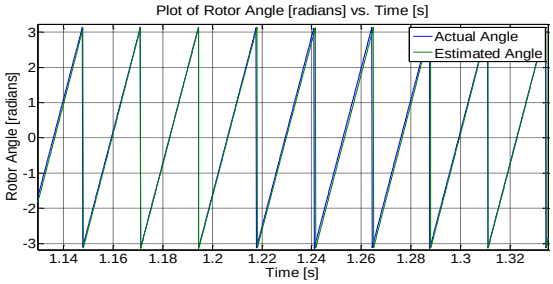

Figure 9: Plot of Rotor Angle [radians] vs. Time [s] in Sensorless mode, i_{Rd}=2.82 A and i_{Rq} = 2.39 A at 1300 rpm.

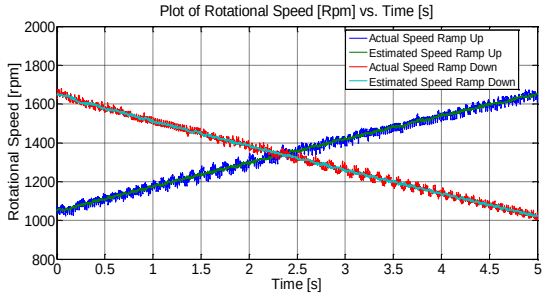

Figure 10: Plot of Rotational Speed [rpm] vs. Time [s] in Sensorless mode, i_{Rd}=2.82 A and i_{Rq} = 2.39 A between 1000 rpm to 1700 rpm.

6 COMMENTS AND CONCULSIONS

The performance of the DFIM under sensored SFO vector control has been shown to be satisfactory as the system currents and powers are able to follow reference inputs (Figures 4 and 5). The suggested values for i_{Rd} and i_{Rq} (rated stator operation) produce a Stator Active Power P equal to the rated value of the DFIM (Table 1). For these references the Stator Reactive Power Q oscillates about a 0 VAr reference in order to have a high power factor close to unity. By using other values than those presented in this paper the Stator Active Power P can be reduced to a fraction of that associated with rated operation, while the Stator Reactive Power Q can be modified to a non-zero value.

The dq-frame rotor currents and the Stator Active/Reactive Power (Figures 6 and 7) in sensorless mode are similar to those observed in sensored mode (Figures 4 and 5). The rotor speed/position estimates (Figure 8 and 9) are similar to the actual values measured through the encoder. The estimated rotational speed (Figure 8) has an erroneous harmonic component superimposed on the actual signal which is introduced through sensor measurements. This harmonic component is also present in an attenuated form in the estimated rotor angle (Figure 9). The nature of the error in the estimates is low, such that encoder measurements can be replaced. The rotor dq-frame currents and stator powers are slightly deteriorated due to the error present in the estimates during changeover to sensorless control, however this effect can be considered negligible.

Given these results the DFIM with SFO vector control, in both sensored and sensorless modes was shown operating with an adequate performance through a wide range of speeds. Hence from the results presented in this paper it was concluded that the algorithms used in this research are suitable for integration with a similar DFIM in a practical WECS.

7 ACKNOWLEDGEMENTS

The research work disclosed in this publication is partially funded by the Strategic Educational Pathways Scholarship (Malta). This Scholarship is part finance by the European Union – European Social Fund (ESF) under Operational Programme II – Cohesion Policy 2007-2013, "Empowering People for More Jobs and a Better Quality Of Life".

8 REFERENCES

[1] World Wind Energy Half-Year Report 2011. Available:http://wwindea.org/home/images/stories/publications/half_year_report_2011_wwea.pdf

[2] E. Tremblay, *et al.*, "Comparative Study of Control Strategies for the Doubly Fed Induction Generation in Wind Energy Conversion Systems: A DSP-Based Implementation Approach," *IEEE Trans. Sustainable Energy*, vol. 2, pp. 288-299, Jul. 2011.

[3] S. Li, *et al.*, "Control of DFIG Wind Turbine Direct-Current Vector Control Configuration," *IEEE Trans. Sustainable Energy*, vol. 3, pp. 1-11, Jan. 2012.
[4] S. Muller, *et al.* (2002, 7th August 2002) Doubly Fed Induction Generator Systems for Wind Turbines. *IEEE Industry Applications Magazine*. 26-33.
[5] K. Spiteri, "Control of a Variable Speed DFIM Using a Matrix Converter," Master of Science in Engineering, University of Malta, Msida, 2009.
[6] R. Pena, *et al.*, "Doubly fed induction generator using back-to-back PWM converters and its application to variable-speed wind-energy generation," *IEE Proc. Electric Power Applications*, vol. 143, pp. 231-241, May 1996.
[7] J. Hu and Y. He, "Dynamic modelling and robust current control of a wind-turbine driven DFIG during external AC voltage drip," *Journal of Zheijang University*, vol. 10, pp. 1757-1764, 2006.
[8] F. Poiters, *et al.* Control of a Doubly-fed Induction Generator for Wind Energy Conversion System. [Technical Article].Available: http://itee.uq.edu.au/~aupec/aupec01/026_%20POITIERS%20_AUPEC01%20paper%20revised.pdf
[9] M. Kayikci and J. V. Milanovic, "Assessing Transient Response of DFIG-Based Wind Palnts - The Influence of Model Simplifications and Parameters," *IEEE Trans. Power Syst.*, vol. 23, pp. 545-554, May 2008.
[10] G. Abad, *et al.*, "Vector Control Strategies for Grid-Connected DFIM Wind Turbines," in *Doubly Fed Induction Machine - Modelling and Control for Wind Energy Generation*, M. E. El-Hawary, Ed., ed New Jersey: John Wiley & Sons, 2011, pp. 303-360.
[11] D. J. Atkinson, *et al.*, "A vector-controlled doubly-fed induction generator for a variable-speed wind turbine application," *Transactions of the Institute of Measurement and Control*, vol. 19, pp. 2-12, Jan. 1997.
[12] K. Spiteri, *et al.*, "Power control of doubly fed induction machine using a rotor side matrix converter," in *Industrial Electronics (ISIE), 2010 IEEE International Symposium on*, 2010, pp. 1445-1450.
[13] K. Spiteri, *et al.*, "Control of doubly fed induction machine using a matrix converter," in *MELECON 2010 - 2010 15th IEEE Mediterranean Electrotechnical Conference*, 2010, pp. 1297-1302.
[14] R. Cardenas, *et al.*, "MRAS Observer for Doubly Fed Induction Machines," *IEEE Trans. Energy Convers.*, vol. 19, Jun. 2004.
[15] R. Cardenas, *et al.*, "MRAS Observers for Sensorless Control of Doubly-Fed Induction Geneartors," *IEEE Trans. Power Electron.*, vol. 23, pp. 1075-1084, May 2008.
[16] R. Cardenas, *et al.*, "MRAS Observer for Sensorless Control of Standalone Doubly Fed Induction Generators," *IEEE Trans. Energy Convers.*, vol. 20, pp. 710-718, Dec. 2005.
[17] M. S. Carmeli, *et al.*, "Effects of Mismatched Parameters in MRAS Sensorless Doubly Fed Induction Machine Drives," *Power Electronics, IEEE Transactions on*, vol. 25, pp. 2842-2851, 2010.
[18] S. M. Gadoue, *et al.*, "MRAS Sensorless Vector Control of an Induction Motor Using New Sliding-Mode and Fuzzy-Logic Adaptation Mechanisms," *Energy Conversion, IEEE Transactions on*, vol. 25, pp. 394-402, 2010.